

Analytical Methods

Accepted Manuscript



This is an *Accepted Manuscript*, which has been through the Royal Society of Chemistry peer review process and has been accepted for publication.

Accepted Manuscripts are published online shortly after acceptance, before technical editing, formatting and proof reading. Using this free service, authors can make their results available to the community, in citable form, before we publish the edited article. We will replace this *Accepted Manuscript* with the edited and formatted *Advance Article* as soon as it is available.

You can find more information about *Accepted Manuscripts* in the [Information for Authors](#).

Please note that technical editing may introduce minor changes to the text and/or graphics, which may alter content. The journal's standard [Terms & Conditions](#) and the [Ethical guidelines](#) still apply. In no event shall the Royal Society of Chemistry be held responsible for any errors or omissions in this *Accepted Manuscript* or any consequences arising from the use of any information it contains.

1
2
3
4 **Magnetic three-dimensional graphene solid-phase extraction coupled**
5 **with high performance liquid chromatography for the determination**
6 **of phthalate esters in fruit juice**
7
8

9
10 Lin Hao, Chenhuan Wang, Xiaoxing Ma, Qiuhua Wu, Chun Wang, Zhi Wang*
11

12
13
14 *College of Science, Agricultural University of Hebei, Baoding 071001, China*
15
16
17
18
19
20
21
22
23

24 Correspondence author: Zhi Wang, College of Science, Agricultural University of
25 Hebei, Baoding 071001, Hebei, China;
26

27
28
29 Tel: +86-312-7521513; Fax: +86-312-7521513;
30

31 E-mail: zhiwang2013@aliyun.com; wangzhi@hebau.edu.cn
32
33
34
35
36
37
38
39
40
41
42
43
44
45
46
47
48
49
50
51
52
53
54

55
56 _____
57 . Corresponding author. Tel.: +86 312 7521513; fax: +86 312 7521513.

58 *E-mail addresses:* zhiwang2013@aliyun.com; wangzhi@hebau.edu.cn
59
60

1
2
3
4
5
6
7
8
9
10
11
12
13
14
15
16
17
18
19
20
21
22
23
24
25
26
27
28
29
30
31
32
33
34
35
36
37
38
39
40
41
42
43
44
45
46
47
48
49
50
51
52
53
54
55
56
57
58
59
60

Abstract: In this paper, a three-dimensional graphene-based magnetic nanocomposite (3D-G-Fe₃O₄), was synthesized and used as an effective adsorbent for the extraction of four phthalate esters (dimethyl(o-)phthalate, diethyl(o-)phthalate, diallyl(o-)phthalate and bis(2-propylheptyl) phthalate) from fruit juice prior to high performance liquid chromatography analysis. The three-dimensional nanoporous structure of the 3D-G endows the new material with a high adsorption capacity. The properties and morphology of the 3D-G-Fe₃O₄ were characterized by transmission electron microscopy, scanning electron microscopy and infrared spectra. Several experimental parameters affecting the extraction efficiencies, such as the amount of the 3D-G-Fe₃O₄, extraction time, sample pH, salt addition and desorption conditions were optimized. Under the optimum conditions, the limits of detection ($S/N = 3$) of the method for the analytes were between 0.04 and 0.13 ng mL⁻¹. The recoveries of the method for the analytes were in the range from 87.0% to 97.8%. The result showed that the 3D-G-Fe₃O₄ has an excellent adsorption capacity for the analytes.

Keywords: Three-dimensional graphene; Magnetic solid phase extraction; High performance liquid chromatography; Phthalate esters; Fruit juice

Introduction

Graphene (G), one-atom-thick planar carbon material patterned in a honeycomb lattice form, is a two-dimensional (2D) carbon nanomaterial and has attracted enormous research interest in recent years owing to its intriguing properties, such as high thermal and electronic conductivity, excellent mechanical strength and high specific surface area^{1,2}. Because the large delocalized π -electron system of G can form a strong hydrophobic and π -stacking interaction with some organic molecules³, it has been widely used as an adsorbent to concentrate many kinds of compounds in various sample pretreatment techniques, such as solid-phase microextraction (SPME)^{4,5}, solid-phase extraction (SPE)^{6,7} and magnetic solid-phase extraction (MSPE)^{8,9}.

However, due to the strong π - π stacking interaction, hydrophobic interaction and van der Waals forces, restacking and aggregation between individual graphene sheets may occur, which may greatly decrease the intrinsic specific surface area of G^{10,11}. In order to overcome the above problems, very recently, Chen et al. have synthesized a three-dimensional interconnected graphene (3D-G) with a foam-like network structure by a chemical vapour deposition method^{12,13}. This structures provide graphene materials with high specific surface areas, strong mechanical strengths, fast mass and electron transport kinetics due to the combination of the 3D porous structures and the excellent intrinsic properties of graphene^{14,15}. 3D-G has been used in the fields of energy storage, biochemical sensing device and stretchable conductors¹⁶⁻¹⁹. Since 3D-G has a high surface area, large mesopore volume and three-dimensional nanoporous structure, it might be a promising candidate for an efficient adsorbent²⁰ for some organic compounds. To the best of our knowledge, the application of 3D-G as the adsorbent for the extraction or removal of organic pollutants was still very few in the literature.

Phthalate esters (PAEs) are widely used in industrial plastics, polyvinyl chloride products, cosmetics and personal care products²¹. Because PAEs are only physically bound to the polymer chains, they can easily leach, migrate or evaporate into various environments during the production, use and incineration of the polymeric materials containing these compounds²². Certain PAEs as well as their metabolites and degradation products can cause adverse effects on human health, especially on the liver, kidney and testicles²³. It has been reported that PAEs are suspected to have carcinogenic and estrogenic properties²⁴. So, for the sake of human health and environment

1
2
3 protection, a sensitive analytical method is necessary for the determination of trace level of PAEs in
4
5 different matrix samples.
6

7 Magnetic solid-phase extraction, as a new mode of SPE, can be carried out directly in crude
8
9 sample solution with the magnetic solid absorbent being added in it and the phase separation can be
10
11 realized simply by using an external magnet without the need of using additional filtration or
12
13 centrifugation procedures, which makes separation easier and faster²⁵⁻²⁸.
14

15 In this report, a three-dimensional graphene-based magnetic nanocomposite (3D-G-Fe₃O₄) was
16
17 synthesized to explore its application potential in MSPE. To evaluate the performance of the
18
19 3D-G-Fe₃O₄, PAEs were selected as the model analytes. After their preconcentration with the
20
21 3D-G-Fe₃O₄, the analytes in fruit juice were determined by high-performance liquid
22
23 chromatography- diode array detection (HPLC-DAD).
24
25
26

27 **Experimental**

31 **Reagents and materials**

32
33 Graphite powder (50 meshes) and FeSO₄·7H₂O were purchased from the Boaxin Chemical
34
35 Reagents Company (Baoding, China). Acetonitrile, methanol, acetone, hydrochloric acid (HCl),
36
37 sodium hydroxide (NaOH), sodium chloride, ammonium hydroxide, and all other reagents were
38
39 purchased from Beijing Chemical Reagents Company (Beijing, China). Dimethyl(o-)phthalate
40
41 (DMP), diethyl(o-)phthalate (DEP), diallylo(o-)phthalate (DAP) and bis(2-propylheptyl) phthalate
42
43 (DPP) were purchased from Aladdin-Reagent (Shanghai, China). The water used throughout the
44
45 work was double-distilled on a SZ-93 automatic double-distiller purchased from Shanghai Yarong
46
47 Biochemistry Instrumental Factory (Shanghai, China). The fruit juice was purchased from local
48
49 supermarket (Baoding, China).

50 A mixture stock solution containing each of DMP, DEP, DPP and DAP at 40.0 μg mL⁻¹ was
51
52 prepared in methanol. A series of standard solutions were prepared by mixing an appropriate
53
54 amount of the stock solution with methanol in a 10-mL volumetric flask. All the standard solutions
55
56 were stored at 4 °C in the dark.
57
58
59
60

Apparatus

The HPLC system, assembled from modular components (Waters, Milford, MA, USA), consisted of an in-line degasser, a 600E pump and a DAD system. A Millennium32 workstation (Waters) was utilized for the control of the system and for the acquisition and analysis of the data. A Centurysil C18 column (250 mm × 4.6 mm id, 5.0 mm) from Dalian Johnson Separation Science Technology Corporation (Dalian, China) was used for separations. The mobile phase was a mixture of acetonitrile–water (65:35 v/v) at a flow rate of 1.0 mL min⁻¹. The UV monitoring wavelength for all the analytes was set at 225 nm.

The size and morphology of the magnetic nanoparticles were observed by transmission electron microscopy (TEM) using a JEOL model JEM-2011(HR) (Tokyo, Japan) at 5 kV and scanning electron microscopy (SEM) using S-3000N microscope (Hitachi, Japan). The infrared spectra (IR) were obtained by a WQF-510 FT-IR Spectrometer (Ruili, China). The Brunauer–Emmett–Teller (BET) surface areas were determined from the N₂ adsorption at 77 K using Tristar 3020 (USA). The magnetic property was analyzed using a JDM-13 vibrating sample magnetometer (VSM, Jilin University, Changchun, China) at room temperature.

Synthesis of 3D-G-Fe₃O₄ and 2D-G-Fe₃O₄

The preparation process of the 3D-G-Fe₃O₄ is illustrated in Scheme 1. Graphene oxide was prepared from natural graphite powders by a modified Hummers' method²⁹. Then, to the 50 mL aqueous suspension of GO at the concentration of 2 mg mL⁻¹, 0.695 g FeSO₄·7H₂O were added, which was sonicated for 5 min. After that, the pH of the resulting mixture was adjusted to 11 with 25% NH₃·H₂O, and the resultant slurry was then heated at 90 °C for 6 hours in an oil bath without stirring. Then, the formed 3D-G-Fe₃O₄ was separated by filtration, washed with water and then freeze-dried under vacuum to remove absorbed water. The reduced graphene oxide sheets anchored with nanoparticles were simultaneously self-assembled into the 3D hydrogel with interconnected networks driven by combined hydrophobic and π-π stacking interactions, due to the decrease of oxygenated groups on the graphene sheets^{30,31}.

Two-dimensional graphene nanocomposite (2D-G-Fe₃O₄) was synthesized according to the method reported in our previous work³². Briefly, GO nanosheets were reduced to 2D-graphene by hydrazine solution. The magnetic (2D-G-Fe₃O₄) was synthesized by the *in situ* chemical

coprecipitation of Fe²⁺ and Fe³⁺ in alkaline solution in the presence of 2D-G.

Scheme 1

MSPE procedures

Firstly, 15.0 mg of 3D-G-Fe₃O₄ was added into a 150 mL aqueous sample solution in a conical flask. Then, the mixture was shaken on a slow-moving platform shaker for 25 min. Then, the 3D-G-Fe₃O₄ was separated from the aqueous phase using a magnet and the resultant supernatant was discarded. After that, the residual solution and 3D-G-Fe₃O₄ were totally transferred to a centrifuge tube. The 3D-G-Fe₃O₄ was aggregated to the bottom of the tube again by positioning a magnet to the outside of the tube wall so that the residual solution could be removed completely using pipette. At last, the isolated 3D-G-Fe₃O₄ nanoparticles were vortexed in 0.2 mL acetone for 1 min for desorption. The desorption was performed in a dry glass centrifuge tube, which has a cap to prevent the evaporation of the desorption solvent. Finally 20 μL desorption solution was injected into the HPLC system for analysis.

Prior to next use, the used 3D-G-Fe₃O₄ nanoparticles were washed three times with 1 mL acetone and then with 1 mL water by vortexing for 1 min, respectively.

In order to evaluate the extraction performance of the method, the extraction recovery (R) was calculated according to the following equation:

$$R\% = \frac{V_{\text{rec}} \cdot C_{\text{inj}}}{C_0 \cdot V_{\text{aq}}}$$

R%, V_{rec} and V_{aq} are the extraction recovery, the volume of the final reconstituted solution and aqueous sample, respectively. C_{rec} and C_0 are the concentration of the analytes in the final reconstituted solution in the extraction and the initial concentration of the analytes in the aqueous sample, respectively.

Results and discussion

Characterization of 3D-G-Fe₃O₄ nanoparticles

1
2
3 In the formation of 3D-G-Fe₃O₄, the Fe²⁺ in FeSO₄·7H₂O was oxidized to Fe³⁺ by the oxygen
4 containing functional groups on the GO nanosheets and simultaneously, the graphene oxide was
5 reduced to graphene by Fe²⁺. Then the formed Fe³⁺ ions and Fe²⁺ ions coprecipitated into Fe₃O₄
6 nanoparticles, which were decorated onto the thin graphene sheets. Simultaneously, the reduced
7 graphene oxide decorated with Fe₃O₄ was self-assembled into the 3D structure with interconnected
8 networks. The reason for that could be ascribed to the partial overlapping or coalescence of the
9 flexible reduced GO nanosheets via noncovalent interactions, such as π-π stacking, hydrogen
10 bonding, and hydrophobic interactions.

11
12 The SEM image of 3D-G-Fe₃O₄ is shown in Fig. 1 (a), from which it can be seen that the
13 so-prepared 3D-G-Fe₃O₄ had a well-defined and interconnected 3D network microstructure. The
14 iron oxide nanoparticles were well distributed on the surface of graphene sheets. The TEM image in
15 Fig. 1 (b) illustrates one of the separated graphene sheets from 3D network and it shows that the
16 Fe₃O₄ nanoparticles were uniformly distributed on the graphene and no particles that were
17 disassociated from the graphene sheets were observed.

18
19 The FTIR spectrum suggests the presence of the functional groups on GO (Fig. 1(c) (GO)). The
20 FTIR bands at 1412, 1060 and 1750 cm⁻¹ are due to the vibrations of O-H, C-O and C=O,
21 respectively. In the IR spectrum for 3D-G-Fe₃O₄, the reduction of GO to G was verified by the
22 vanished band at 1060 and 1750 cm⁻¹, which indicated that the characteristic epoxy and carboxyl
23 vibrational bands have disappeared. Moreover, the peak at 600 cm⁻¹ can be ascribed to lattice
24 absorption of iron oxide.

25
26 Fig. 1(d) shows the N₂ adsorption-desorption isotherms of 3D-G-Fe₃O₄. The Brunauer-Emmett-
27 Teller (BET) specific surface area of 3D-G-Fe₃O₄ is about 308.1 m² g⁻¹, which is superior to the
28 2D-G-Fe₃O₄ (~225.0 m² g⁻¹²⁸).

29
30 It is important that the adsorbents possess superparamagnetic properties to realize rapid
31 separation under a magnetic field. Fig. 2 shows the VSM magnetization curves of the 3D-G-Fe₃O₄
32 nanoparticles at 298 K. It exhibited typical superparamagnetic behavior. The saturation
33 magnetization intensity of 3D-G-Fe₃O₄ was 39.5 emu g⁻¹, which are sufficient for its magnetic
34 separation from a solution with a strong magnet.

35
36
37
38
39
40
41
42
43
44
45
46
47
48
49
50
51
52
53
54
55
56
57
58
59
60

Fig. 1

Fig. 2

Optimization of extraction conditions

In order to obtain the optimum conditions, 150 mL double-distilled water spiked with 40.0 ng mL^{-1} each of the four PAEs was used to study the extraction performance of the 3D-G- Fe_3O_4 under different experimental conditions. The experimental parameters investigated included the amount of 3D-G- Fe_3O_4 , extraction time, sample pH, ionic strength, and desorption conditions. All the experiments were performed in triplicate and the means of the results were used for optimization.

Effect of the amount of 3D-G- Fe_3O_4 sorbents

To investigate the performance of 3D-G- Fe_3O_4 , its adsorption ability for the PAEs was compared with that of both 2D-G- Fe_3O_4 and Fe_3O_4 . The results shown in Fig. 3 indicated that the extraction efficiency of 3D-G- Fe_3O_4 was higher than that obtained by either 2D-G- Fe_3O_4 or Fe_3O_4 under the same conditions. This could be attributed to the high specific surface area and three-dimensional nanoporous structure of 3D-G- Fe_3O_4 . Based on the above results, the 3D-G- Fe_3O_4 was selected as adsorbent for the extraction of the three PAEs.

In order to select the optimum dosage of the 3D-G- Fe_3O_4 for the extraction of the PAEs, different amounts of the 3D-G- Fe_3O_4 were investigated in the range from 2 to 20 mg. The results (Fig. 4) shows that the adsorption for all the four PAEs could reach the maximum plateau when the dosage of 3D-G- Fe_3O_4 was increased to 10 mg and then remained almost constant. In order to ensure that the adsorbent was sufficient for the extraction, 15 mg 3D-G- Fe_3O_4 was selected.

Fig.3

Fig.4

Effect of extracting time

Extraction time is another important parameter that influences the extraction of the analytes. To investigate the influence of the extraction time on the extraction efficiency, the extraction time was varied in the range from 10 to 40 min. As shown in Fig. 5, the peak areas for all the PAEs reached their maxima when the extraction time was increased to 20 min. In order to ensure that all the PAEs

1
2
3 can achieve their extraction equilibrium, an extraction time of 25 min was chosen.
4
5

6
7
8
9
10
11
12
13
14
15
16
17
18
19
20
21
22
23
24
25
26
27
28
29
30
31
32
33
34
35
36
37
38
39
40
41
42
43
44
45
46
47
48
49
50
51
52
53
54
55
56
57
58
59
60

Fig. 5

Effect of sample pH

The pH of sample solution is a key factor affecting the extraction efficiency. Since it not only affects the existence forms of the analytes but also changes the charge type and density on the surface of the adsorbent³³. In this study, the effect of pH of the sample solution was investigated in the range from 2.0 to 12.0. The experimental results (Fig. 6) showed that the adsorption efficiency was almost not changed when the pH of the sample solution was changed from 2 to 6 and then decreased rapidly when the pH was further increased. The reason for this is that when the pH of the sample solution exceeds 7, the phthalates could hydrolyze to phthalate anions, which were soluble in aqueous solution³⁴. Considering that the pH of the juice samples investigated was in the range of 5-6, the pH of sample solution was not adjusted.

Fig. 6

Effect of sample salinity

In this study, the effect of salt addition was investigated by changing the concentrations of NaCl from 0% to 3.0%, 5.0%, 10.0%, 15.0% , 20.0% (w/v), respectively. The results showed that the addition of NaCl had a negligible effect on the extraction efficiency for the analytes in the concentration range investigated. Therefore, no NaCl was added to the samples in all the subsequent experiments.

Desorption conditions

In this work, acetonitrile, methanol and acetone were tested as the desorption solvent. As shown in Fig. 7, acetone provided the best desorption efficiency among the three solvents. Therefore, acetone was chosen as the desorption solvent. The effect of the volume of acetone on desorption efficiency was also investigated. The results showed that the analytes could be desorbed quantitatively when the volume of acetone was 200 μ L. Therefore, 200 μ L acetone was selected for desorption.

Fig. 7

Reusability of the sorbent

The reusability of the adsorbent was investigated in this study. After desorption of the analytes from the adsorbent, the used 3D-G-Fe₃O₄ was washed three times each with 1 mL acetone and then with 1 mL water by vortexing for 1 min, respectively. After such washings, no carry-over of the analytes from the adsorbent was detected. The results indicated that the 3D-G-Fe₃O₄ could be reused at least 20 times without significant loss of its adsorption capacity.

Linearity and limits of detection (LODs) of the method

A series of PAEs-free fruit juice samples containing each of the PAEs at seven concentrations (0.2, 0.5, 1.0, 5.0, 20.0, 50.0, 100.0 ng mL⁻¹) were prepared for the establishment of the calibration curve. For each concentration level, four replicate extractions and determinations were performed under the optimized experimental conditions. Good linearity was observed over the concentration range of 0.10-100.0 ng mL⁻¹ for the four PAEs, with the correlation coefficients (*r*) ranging from 0.9905 to 0.9997. The LODs (*S/N*=3) of the method were in the range from 0.042 to 0.060 ng mL⁻¹ for fruit juice samples. The results are listed in Table 1.

Table 1

Sample analysis and recoveries of the method

In order to assess the precision and accuracy of the method, the method was applied to determine the PAEs in different fruit juice samples. The results are shown in Table 2. As a result, 0.34 ng mL⁻¹ of DMP was found in fruit juice sample 1 and no residues of the PAEs were detected in fruit juice 2. To determine the recoveries of the method, the fruit juice samples were spiked with the PAE standards at the concentrations of 5.0 and 10.0 ng mL⁻¹, respectively. The recoveries for the PAEs in fruit juice samples are listed in Table 2. The results indicated that the recoveries were in the range from 87.0% to 97.8% with RSDs between 3.3% and 5.1%. Fig. 8 shows the typical chromatograms of fruit juice sample before and after being spiked with each of the PAEs at 5.0 ng mL⁻¹.

Fig. 8

Table 2

Conclusions

In this report, a three-dimensional graphene magnetic nanomaterial was prepared and used as an effective adsorbent for the first time. After adsorption of the PAEs from fruit juice by 3D-G-Fe₃O₄, the PAEs were desorbed and then determined by HPLC-DAD. Because of the 3D porous structures, high specific surface area and strong magnetism of the 3D-G-Fe₃O₄, it shows an excellent adsorption capacity for the analytes. The developed method is efficient and easy to be used, without the need of additional centrifugation or filtration procedures. The results suggest that the 3D-G-Fe₃O₄ should have more applications for the effective extractions of other compounds.

Acknowledgements

Financial supports from the National Natural Science Foundation of China (No. 31171698), the Innovation Research Program of Department of Education of Hebei for Hebei Provincial Universities (LJRC009), the Natural Science Foundations of Hebei (B2012204028) and the Scientific and Technological Research Foundation of Department of Education of Hebei Province (ZD20131033) are gratefully acknowledged.

References

1. D. A. C. Brownson and C. E. Banks, *Electrochem. Commun.*, 2011, **13**, 111-113.
2. J. Chen, J. Zou, J. Zeng, X. Song, J. Ji, Y. Wang, J. Ha and X. Chen, *Anal. Chim. Acta*, 2010, **678**, 44-49.
3. T. V. Cuong, V. H. Pham, Q. T. Tran, J. S. Chung, E. W. Shin, J. S. Kim and E. J. Kim, *Mater. Lett.*, 2010, **64**, 765-767.
4. Q. Liu, J. Shi and G. Jiang, *TrAC, Trends Anal. Chem.*, 2012, **37**, 1-11.
5. Y. Ke, F. Zhu, F. Zeng, T. Luan, C. Su and G. Ouyang, *J. Chromatogr. A*, 2013, **1300**, 187-192.
6. Y. B. Luo, B. F. Yuan, Q. W. Yu and Y. Q. Feng, *J. Chromatogr. A*, 2012, **1268**, 9-15.
7. Q. Liu, J. Shi, L. Zeng, T. Wang, Y. Cai and G. Jiang, *J. Chromatogr. A*, 2011, **1218**, 197-204.
8. G. Zhao, S. Song, C. Wang, Q. Wu and Z. Wang, *Anal. Chim. Acta*, 2011, **708**, 155-159.
9. S. Zeng, N. Gan, R. Weideman-Mera, Y. Cao, T. Li and W. Sang, *Chem. Eng. J.*, 2013, **218**, 108-115.

10. C. Li and G. Shi, *Nanoscale*, 2012, **4**, 5549-5563.
11. S. Nardecchia, D. Carriazo, M. L. Ferrer, M. C. Gutiérrez and F. del Monte, *Chem. Soc. Rev.*, 2013, **42**, 794-830.
12. Z. Chen, W. Ren, L. Gao, B. Liu, S. Pei and H. M. Cheng, *Nat. Mater.*, 2011, **10**, 424-428.
13. X. Wang, Y. Zhang, C. Zhi, X. Wang, D. Tang, Y. Xu, Q. Weng, X. Jiang, M. Mitome, D. Golberg and Y. Bando, *Nat. Commun.*, 2013, **4**, 2905.
14. C. Li and G. Shi, *Nanoscale*, 2012, **4**, 5549-5563.
15. J. S. Cheng, J. Du and W. Zhu, *Carbohydr. Polym.*, 2012, **88**, 61-67.
16. W. Wang, S. Guo, M. Penchev, I. Ruiz, K. N. Bozhilov, D. Yan, M. Ozkan and C. S. Ozkan, *Nano Energy*, 2013, **2**, 294-303.
17. V. C. Tung, L. M. Chen, M. J. Allen, J. K. Wassei, K. Nelson, R. B. Kaner and Y. Yang, *Nano Lett.*, 2009, **9**, 1949-1955.
18. G. Ning, T. Li, J. Yan, C. Xu, T. Wei and Z. Fan, *Carbon*, 2013, **54**, 241-248.
19. A. L. Liu, G. X. Zhong, J. Y. Chen, S. H. Weng, H. N. Huang, W. Chen, L. Q. Lin, Y. Lei, F. H. Fu, Z. L. Sun, X. H. Lin, J. H. Lin and S. Y. Yang, *Anal. Chim. Acta*, 2013, **767**, 50-58.
20. H. Liu, Y. Wang, X. Gou, T. Qi, J. Yang and Y. Ding, *Mater. Sci. Eng., B*, 2013, **178**, 293-298.
21. X. Wu, H. Hong, X. Liu, W. Guan, L. Meng, Y. Ye and Y. Ma, *Sci. Total Environ.*, 2013, **444**, 224-230.
22. C. A. Stales, D. R. Peterson, T. F. Parkerton and W. J. Adams, *Chemosphere*, 1997, **35**, 667-749.
23. P. Serodio and J. M. Nogueira, *Water Res.*, 2006, **40**, 2572-2582.
24. F. J. López-Jiménez, S. Rubio and D. Pérez-Bendito, *Anal. Chim. Acta*, 2005, **551**, 142-149.
25. S. S. Bai, Z. Li, X. H. Zang, C. Wang and Z. Wang, *Chin. J. Anal. Chem.*, 2013, **41**, 1177-1182.
26. W. Huang, J. Ding and Y. Q. Feng, *Chin. J. Anal. Chem.*, 2012, **40**, 830-834.
27. I. S. Ibarra, J. A. Rodriguez, J. M. Miranda, M. Vega and E. Barrado, *J. Chromatogr. A*, 2011, **1218**, 2196-2202.
28. W. Wang, Y. Li, Q. Wu, C. Wang, X. Zang and Z. Wang, *Anal. Methods*, 2012, **4**, 766-772.
29. T. Nakajima, A. Mabuchi and R. Hagiwara, *Carbon*, 1988, **26**, 357-361.
30. H. P. Cong, X. C. Ren, P. Wang and S.-H. Yu, *Acs Nano*, 2012, **6**, 2693-2703.
31. Z. Tang, S. Shen, J. Zhuang and X. Wang, *Angew. Chem. Int. Ed.*, 2010, **122**, 4707-4711.

1
2
3 32. C. Wang, C. Feng, Y. Gao, X. Ma, Q. Wu and Z. Wang, *Chem. Eng. J.*, 2011, **173**, 92-97.
4

5 33. G. Zhao, S. Song, C. Wang, Q. Wu and Z. Wang, *Anal. Chim. Acta*, 2011, **708**, 155-159.
6

7 34. J. Li, Q. Su, K. Y. Li, C. F. Sun and W. B. Zhang, *Food Chem.*, 2013, **141**, 3714-3720.
8
9
10
11
12
13
14
15
16
17
18
19
20
21
22
23
24
25
26
27
28
29
30
31
32
33
34
35
36
37
38
39
40
41
42
43
44
45
46
47
48
49
50
51
52
53
54
55
56
57
58
59
60

Table Captions

Table 1 Analytical performance data for the PAEs by the MSPE technique.

Table 2 Determination of the phthalate esters and recoveries in fruit juice samples.

Scheme Captions

Scheme 1 Schematic illustration of synthetic processes of the 3D-G-Fe₃O₄

Figure Captions

Fig. 1. The SEM and TEM images of 3D-G-Fe₃O₄

Fig. 2. VSM magnetization curves of 3D-G-Fe₃O₄

Fig. 3. Comparisons of the adsorption performance of 3D-G-Fe₃O₄ with 2D-G-Fe₃O₄ and Fe₃O₄ for the extraction of the four PAEs

Fig. 4. Effect of the amount of the adsorbent on the extraction efficiency of the PAEs

Fig. 5. Effect of extraction time on the extraction efficiency of the PAEs.

Fig. 6. Effect of pH on the extraction efficiency of the PAEs.

Fig. 7. Effect of the desorption solvent on the extraction efficiency of the PAEs.

Fig. 8. The typical chromatograms of fruit juice sample (a) and the fruit juice sample spiked with the PAEs at each concentration of 5.0 ng mL⁻¹ (b). Peak identifications: 1. DMP, 2. DEP, 3. DAP, 4. DPP

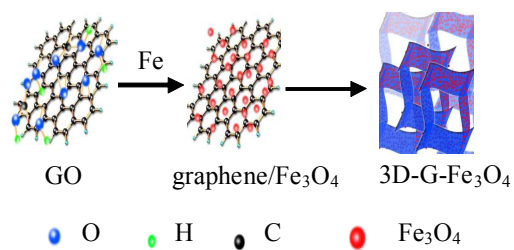
Table 1 Analytical performance data for the PAEs by the MSPE technique.

PAEs	Linear range (ng mL ⁻¹)	<i>r</i>	RSD (%)	LOD (ng mL ⁻¹)
DMP	0.1-100.0	0.9996	3.3	0.042
DEP	0.1-100.0	0.9930	4.8	0.050
DAP	0.1-100.0	0.9997	3.3	0.042
DPP	0.1-100.0	0.9985	3.8	0.060

Table 2 Determination of phthalate esters and recoveries in fruit juice samples

PAEs	Spiked (ng mL ⁻¹)	Fruit juice sample 1			Fruit juice sample 2		
		Found (ng mL ⁻¹)	R ^b (%)	RSD (%)	Found (ng mL ⁻¹)	R ^b (%)	RSD (%)
	0.0	0.58			nd ^a		
DMP	5.0	5.37	95.8	5.9	4.50	90.0	5.5
	10.0	10.56	99.8	4.3	9.20	92.0	3.7
	0.0	nd ^a			nd ^a		
DEP	5.0	4.88	97.6	3.6	4.38	87.6	3.1
	10.0	9.60	96.0	4.4	8.86	88.6	4.5
	0.0	nd ^a			nd ^a		
DAP	5.0	4.35	87.0	4.1	4.72	94.4	4.9
	10.0	8.99	89.9	6.2	9.24	92.4	4.2
	0.0	nd ^a			nd ^a		
DPP	5.0	4.87	97.4	4.5	4.84	96.8	5.8
	10.0	9.78	97.8	5.2	9.10	91.0	3.4

^a nd: not detected.; ^b R: recovery of the method.



Scheme 1 Schematic illustration of the synthetic processes of the 3D-G-Fe₃O₄

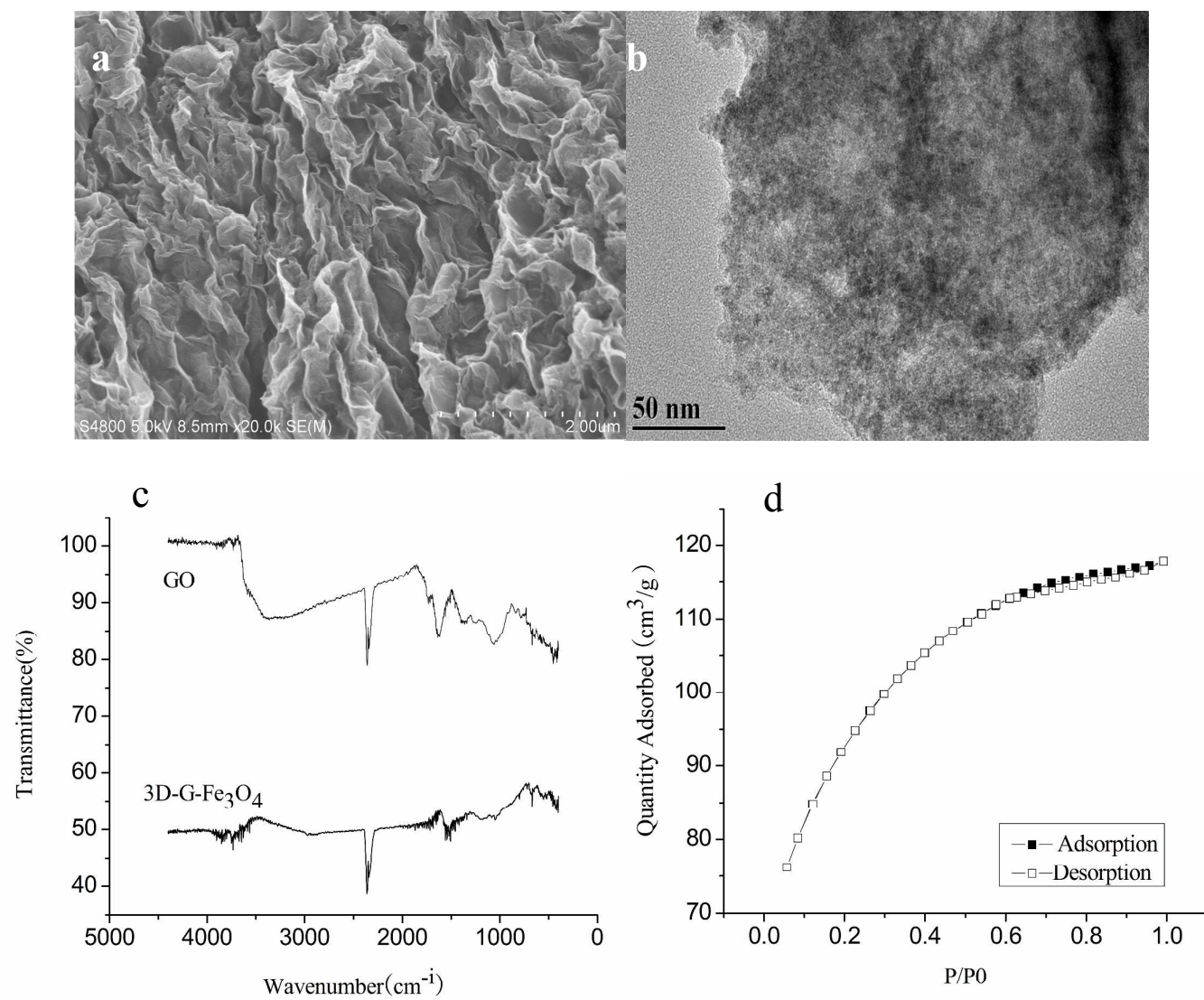


Fig. 1 The SEM (a) and TEM (b) images of 3D-G-Fe₃O₄, FTIR (c) of 3D-G-Fe₃O₄, the N₂ adsorption–desorption isotherms (d) of 3D-G-Fe₃O₄.

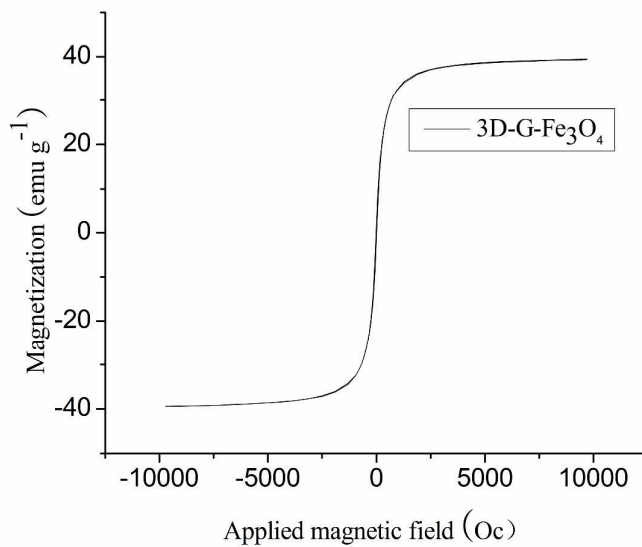


Fig. 2 VSM magnetization curves of 3D-G-Fe₃O₄.

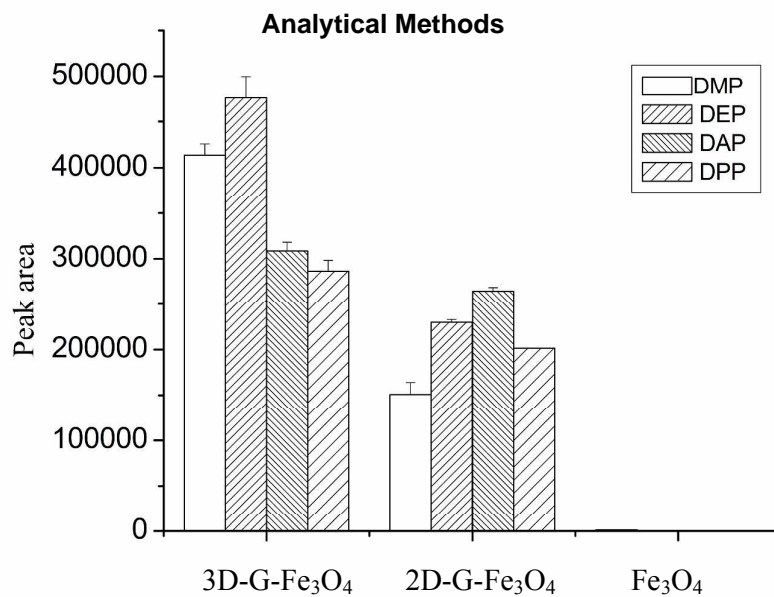


Fig. 3 Comparisons of the adsorption performance of 3D-G-Fe₃O₄ with 2D-G-Fe₃O₄ and Fe₃O₄ for the extraction of the four PAEs.

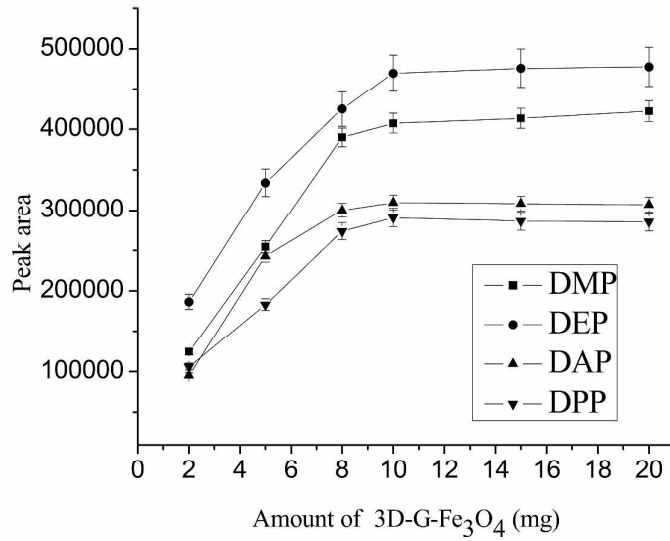


Fig. 4 Effect of the amount of the sorbents on the extraction efficiency of the PAEs.

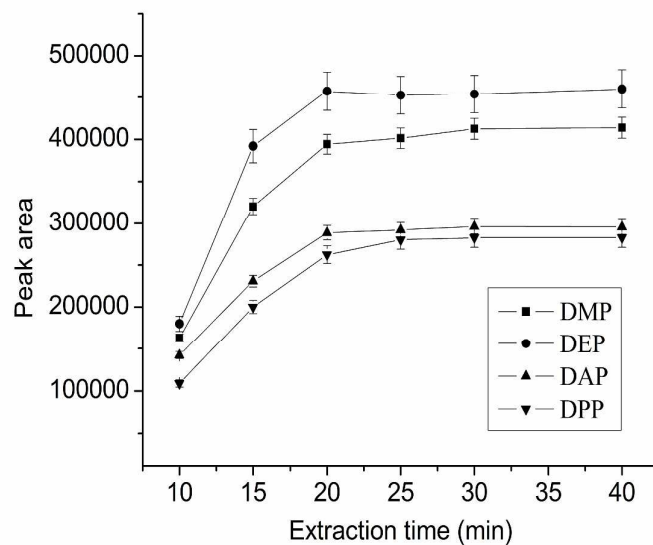


Fig. 5 Effect of extraction time on the extraction efficiency of the PAEs.

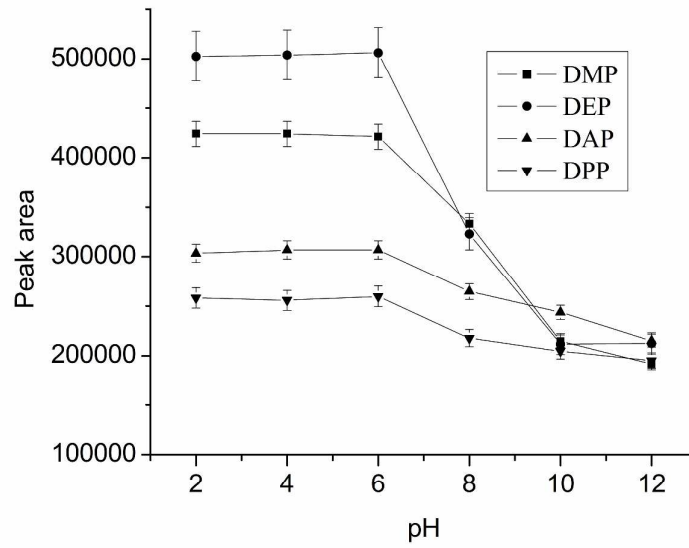


Fig. 6 Effect of pH on the extraction efficiency of the PAEs.

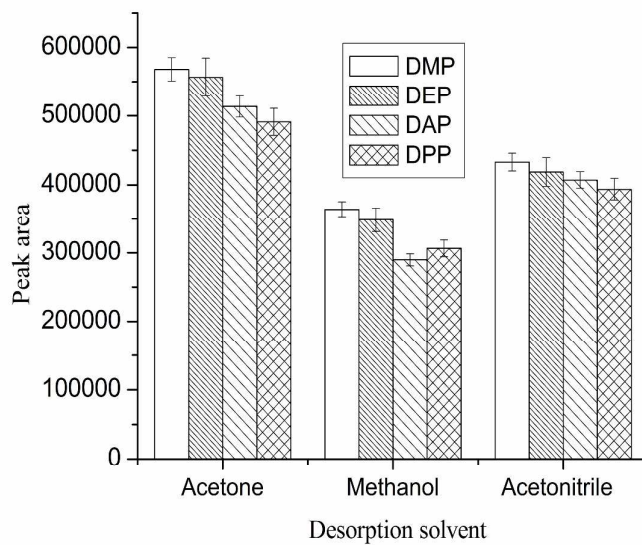


Fig. 7 Effect of the desorption solvent on the extraction efficiency of the PAEs.

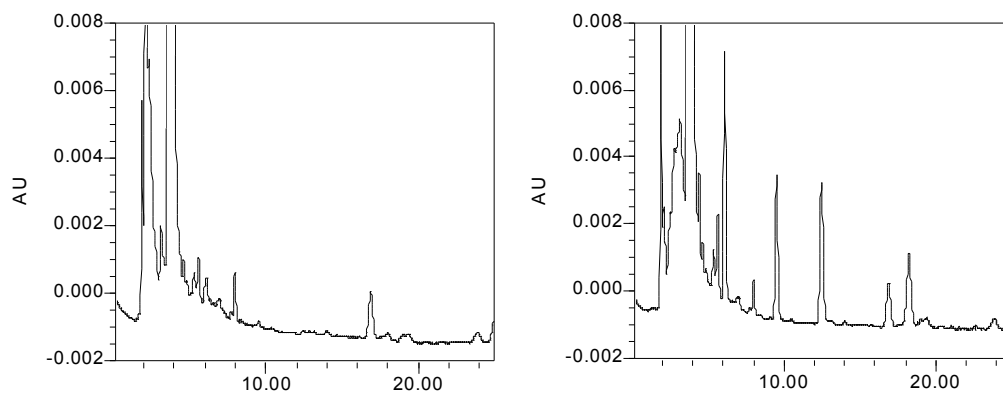


Fig. 8 The typical chromatograms of fruit juice sample (a) and the fruit juice sample spiked with the PAEs at each concentration of 5.0 ng mL^{-1} (b). Peak identifications: 1. DMP, 2. DEP, 3. DAP, 4. DPP.

Self-assembled

Magnetic three-dimensional graphene solid-phase extraction coupled with high performance liquid chromatography for the determination of phthalate esters in fruit juice

Lin Hao, Chenhuan Wang, Xiaoxing Ma, Qiuhua Wu, Chun Wang, Zhi Wang*

College of Science, Agricultural University of Hebei, Baoding 071001, China

In this paper, a novel nanomaterial, three-dimensional graphene-based magnetic nanocomposite (3D-G-Fe₃O₄), was synthesized and used as an effective adsorbent for the extraction of four phthalate esters (dimethyl(o-)-phthalate, diethyl(o-)-phthalate, diallylo(o-)-phthalate and bis(2-propylheptyl) phthalate) from fruit juice prior to high performance liquid chromatography analysis.

